

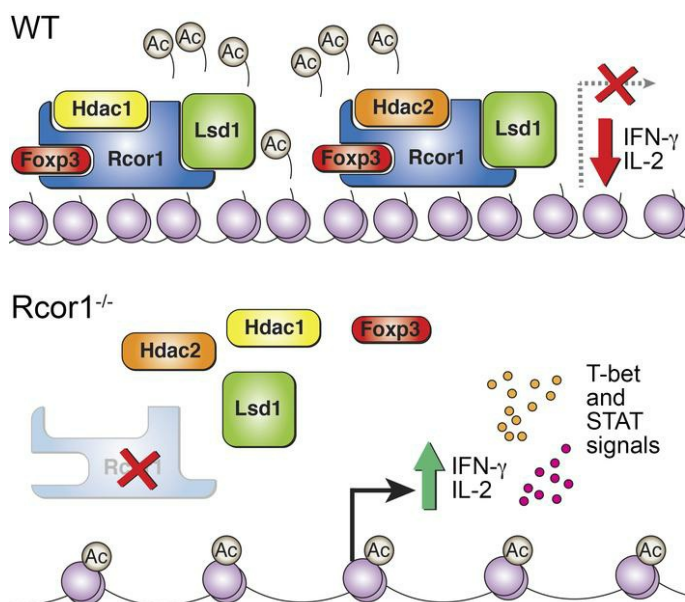
Inhibiting the coregulator CoREST impairs Foxp3⁺ Treg function and promotes antitumor immunity

Yan Xiong, ... , Philip A. Cole, Wayne W. Hancock

J Clin Invest. 2020. <https://doi.org/10.1172/JCI131375>.

Research In-Press Preview Immunology Oncology

Graphical abstract



Find the latest version:

<https://jci.me/131375/pdf>



**Inhibiting the coregulator CoREST impairs Foxp3+ Treg function and promotes
antitumor immunity**

Yan Xiong,^{1,2} Liqing Wang,² Eros Di Giorgio,^{2,3} Tatiana Akimova,² Ulf H. Beier,⁴ Rongxiang Han,²
Matteo Trevisanut,^{2,3} Jay H. Kalin,⁵ Philip A. Cole,⁵ and Wayne W. Hancock²

¹Institute of Hepatobiliary Diseases of Wuhan University, Transplant Centre of Wuhan University,
Zhongnan Hospital of Wuhan University, Wuhan University, Wuhan, China.

²Division of Transplant Immunology, Department of Pathology and Laboratory Medicine,
Children's Hospital of Philadelphia and Perelman School of Medicine, University of Pennsylvania,
Philadelphia, Pennsylvania, USA.

³Department of Medicine, Università degli Studi di Udine, P.le Kolbe 4, Udine, Italy.

⁴Division of Nephrology, Department of Pediatrics, Children's Hospital of Philadelphia and Perelman School of
Medicine, University of Pennsylvania, Philadelphia, Pennsylvania, USA.

⁵Departments of Medicine and Biological Chemistry and Molecular Pharmacology, Harvard Medical School
and Division of Genetics, Brigham and Women's Hospital, Boston, Massachusetts, USA.

Conflict of interest:

The authors have declared that no conflict of interest exists.

Correspondence:

Wayne W. Hancock, Children's Hospital of Philadelphia, 916B Abramson Research Center, 3615 Civic Ctr
Blvd, Philadelphia, Pennsylvania 19104. Phone: 215-590-8709; Email: whancock@penmedicine.upenn.edu

Abstract

Foxp3⁺ T-regulatory (Treg) cells are key to immune homeostasis, but the contributions of various large, multiprotein complexes that regulate gene expression remain unexplored. We analyzed the role in Tregs of the evolutionarily conserved CoREST complex consisting of a scaffolding protein, Rcor1 or Rcor2, plus Hdac1 or Hdac2 and Lsd1 enzymes. Rcor1, Rcor2 and Lsd1 were physically associated with Foxp3, and mice with conditional deletion of Rcor1 in Foxp3⁺ Tregs had decreased proportions of Tregs in peripheral lymphoid tissues, and increased Treg expression of IL-2 and IFN- γ compared to WT cells. Mice with conditional deletion of the gene encoding Rcor1 in their Tregs had reduced suppression of homeostatic proliferation, inability to maintain long-term allograft survival despite costimulation blockade, and enhanced antitumor immunity in syngeneic models. Comparable findings were seen in WT mice treated with CoREST complex bivalent inhibitors, which also altered the phenotype of human Tregs and impaired their suppressive function. Our data point to the potential for therapeutic modulation of Treg functions by pharmacologic targeting of enzymatic components of the CoREST complex, and contribute to an understanding of the biochemical and molecular mechanisms by which Foxp3 represses large gene sets and maintains the unique properties of this key immune cell.

Introduction

T-regulatory (Treg) cells are essential for maintenance of immune homeostasis and self-tolerance (1, 2). These cells also dampen host antitumor immunity, decreasing the efficacy of tumor immune surveillance (3). The key transcription factor Foxp3 has a critical role in the differentiation and function of Treg cells (4, 5), and knockdown or mutations of Foxp3 attenuate the immunosuppressive capacity of Treg cells (6, 7). Similarly, depletion of Foxp3⁺CD4⁺ Treg cells results in severe autoimmunity in otherwise normal animals, and can be reversed by reconstituting Treg cells (8, 9). Recent successes with checkpoint inhibitor therapies in the treatment of various cancers have rekindled interests in immunotherapy. However, despite a major contribution of Foxp3⁺ Treg cells to establishing and maintaining an immunosuppressive tumor microenvironment, there are very few options to selectively target Foxp3⁺ Tregs cells and promote antitumor immunity (10).

REST corepressor 1 (Rcor1 or CoREST) is a protein that binds to the C-terminal domain of REST and regulates diverse immune and inflammatory responses (11). Rcor1 is best known as a core component of the chromatin-modifying CoREST repressor complex (12), that also includes histone deacetylase 1 or 2 (Hdac1/2) (13-15), and the histone 3 lysine 4 (H3K4) demethylase Lsd1 (Kdm1a) (16, 17). HDAC1/2 remove acetyl groups from histone tails and Lsd1 removes monomethylation and/or dimethylation marks from H3K4 (18). Much attention has been focused on understanding the biochemical functions of Rcor1 in various tissues. In patients with diffuse large B-cell lymphoma, deletions in Rcor1 are associated with unfavorable progression-free survival (19). Rcor1 also recruits the INSM1/Rcor1/2 complex, controlling the balance of proliferation and differentiation during brain development (20). In hematopoietic stem cells, loss of Rcor1 in adults leads to a complete block in erythroid and neutrophil differentiation (21). While Rcor1 functions as an epigenetic and repressive factor in immune cells, its role in the regulation of Foxp3⁺ Treg cells has not been studied. Accordingly, we conditionally deleted Rcor1 in Tregs, and tested the effects of recently characterized dual Hdac1/2 and Lsd1 (CoREST) inhibitors. We found that gene deletion or pharmacologic inhibition disrupted Foxp3-dependent recruitment of the CoREST complex to the promoters of T-bet, IL-2 and IFN- γ , leading to Treg production of IL-2 and IFN- γ , impaired Treg function and enhanced anti-tumor immunity.

Results

Foxp3, Rcor1 and the CoREST complex. Foxp3 has a central role in maintaining Treg stability and function, and forms multiprotein complexes (≥ 400 -800 kDa) that include various transcription factors and repressor complexes (22), though the functions of these evolutionarily highly conserved repressor complexes are largely unexplored. We analyzed the roles in Tregs of the CoREST scaffolding proteins, Rcor1 and Rcor2, and their associated enzymes Hdac1, Hdac2 and Lsd1. In 293T cells transfected with tagged constructs, immunoprecipitation (IP) of Foxp3 lead to co-IP of Rcor1 (44 kDa) but not Rcor2 (53 kDa, Figure 1A). In reciprocal studies, IP of Rcor1 led to co-IP of Foxp3, as well as Rcor2 and p300 (Figure 1B). We have previously shown that IP of Foxp3 leads to co-IP of p300, which is important for Foxp3 acetylation, dimerization and Treg function (23). The association of Rcor1 with Foxp3 was also demonstrated using Tregs; IP of Rcor1 led to co-IP of Foxp3 (Figure 1C), and IP of Foxp3 led to co-IP of Rcor1 (Figure 1D). Hence, Rcor1 can associate with Foxp3, and with Rcor2 as part of the CoREST complex.

We next conditionally deleted *Rcor1* in Foxp3⁺ Treg cells by crossing *Rcor1^{fl/fl}* and Foxp3^{YFP/Cre} mice (Figure 1E). *Rcor1^{fl/fl}Foxp3^{YFP/Cre}* (hereafter *Rcor1^{-/-}*) mice were born at expected Mendelian ratios and, upon monitoring for up to 1 year, developed normally, without development of weight loss, dermatitis, lymphadenopathy, splenomegaly, histologic abnormalities or other evidence of autoimmunity. To test whether Treg deletion of *Rcor1* affected Foxp3 association with the CoREST complex, we undertook IP of Lsd1 and Western blotting of immunoprecipitates for Foxp3. Unlike in WT Tregs, the association of Foxp3 with the Lsd1 was largely lost in *Rcor1^{-/-}* Tregs (Figure 1F).

To further characterize the *Rcor1^{-/-}* mice, secondary lymphoid tissues were harvested, single cell suspensions prepared, and cell populations and activation markers assessed by flow cytometry. *Rcor1^{-/-}* mice showed moderately decreased proportions of Foxp3⁺CD4⁺ Tregs within lymph nodes and spleen (Figure 2A), and there were only a few significant differences in basal T cell activation makers in lymph nodes, spleen or thymus, including increased proportions of splenic CD69⁺CD8⁺ T cells, decreased proportions of splenic CD4⁺CD69⁺ T cells, and increased levels of CD44^{hi}CD62L^{lo} CD8⁺ in lymph nodes (Figure 2B). The in vitro suppressive

functions of Tregs from $Rcor1^{-/-}$ mice were significantly (though modestly) impaired ($p < 0.05$) compared to WT Tregs (Figure 2C, quantified in Supplemental Figure 1). Hence, Foxp3 can associate with Rcor1 and Lsd1 components of the CoREST complex, and under basal conditions, Rcor1 deletion leads to decreases in peripheral Treg numbers and Treg suppressive function in vitro.

We wondered whether the lack of a phenotype under steady-state conditions in the $Rcor1^{-/-}$ mice might reflect compensation by Rcor2, and briefly explored this by developing mice with conditional deletion of Rcor2 ($Rcor2^{fl/fl}Foxp3^{YFP/Cre}$), or both Rcor1 and Rcor2 ($Rcor1^{fl/fl}Rcor2^{fl/fl}Foxp3^{YFP/Cre}$), in their Tregs. Conditional deletion of Rcor2 led to a similar small decrease in peripheral Treg proportions in peripheral lymphoid tissues as seen with Rcor1 deletion (Supplemental Figure 2A). However, in contrast to Rcor1, deletion of Rcor2 led to a modest increase ($p < 0.05$) in Treg suppressive function (Supplemental Figure 2B). Dual deletion of Rcor1 and Rcor2 decreased thymic Treg production, and their peripheral Tregs had somewhat impaired Treg function ($p < 0.05$) like seen with Rcor1 deletion (Supplemental Figure 2A, B). Under steady-state conditions, deletions of Rcor1, Rcor2, or both Rcor1 and Rcor2 in Tregs did not lead to marked changes in activation of CD4 or CD8 T cells (Supplemental Figure 2C). These data, while not exhaustive, suggest that Rcor1 plays a dominant role in Tregs that is not able to be duplicated by Rcor2.

Profound effects of Rcor1 deletion on gene expression in Tregs and derepression of IL-2 and IFN- γ . We undertook RNA-seq analyses of $Rcor1^{-/-}$ and WT Tregs to assess Rcor1-dependent global changes in gene expression. There were 1074 genes downregulated and 816 genes upregulated in Rcor1 KO Treg (>2 -fold, $p < 0.05$) compared with WT Treg (Figure 3A). A hierarchical clustering map for differential gene expression is shown in Supplemental Figure 3. Differentially expressed genes included cytokines and chemokines (Figure 3B), leukocyte antigens (Figure 3C) and transcription factors (Figure 3D). Upregulation of various genes of interest, including IL-2, IL-4, IL-10, IFN- γ , Stat1, Stat4, Tbox1, CD73, CTLA4, Ebi3, ICOS and CD25, was confirmed by qPCR (Figure 3E and Supplemental Figure 4), as well as by flow cytometric analysis of cytokine production by activated Treg cells (Supplemental Figure 5). Functional annotation clustering also showed enrichment of genes associated with inflammatory and immune responses in $Rcor1^{-/-}$ vs. WT Tregs (Figure 3F).

Treg expression of cytokines such as IL-2 and IFN- γ is normally highly suppressed, and epigenetic mechanisms are thought to significantly contribute to such regulation. Hence, we used ChIP analysis to assess chromatin remodeling at relevant gene promoters as a result of *Rcor1* deletion. We pulled down chromatin with anti-Lsd1, Hdac1, Hdac2 and acetylated-Histone3 antibodies and analyzed levels of the promoters of IL-2, IFN- γ and T-bet by qPCR. Compared with WT Tregs, *Rcor1*^{-/-} Tregs had dramatic decreases of Hdac2 and LSD1, no significant difference in HDAC1, and a marked increase of ac-Histone3 at the IL-2 promoter (Figure 4A). Likewise, *Rcor1*^{-/-} Tregs showed decreased Lsd1/Hdac1/Hdac2 and increased ac-Histone3 binding at the IFN- γ promoter (Figure 4B). IFN- γ is a signature cytokine of CD4⁺ Th1 cells and its expression is regulated by T-bet (Tbox1). *Rcor1*^{-/-} Tregs showed decreased Hdac1/Hdac2 and increased ac-Histone3 at the T-bet promoter, but there was no significant difference in Lsd1 (Figure 4C). Recent studies have highlighted the cross-regulation of IFN- γ and STAT1 with β -catenin, including in dysfunctional Foxp3⁺ Treg cells (24, 25). Although *Rcor1*^{-/-} Tregs did not affect expression of T-bet and β -catenin proteins under basal conditions, their protein levels were significantly increased in *Rcor1*^{-/-} Tregs upon activation by CD3/CD28 mAb-coated beads for 24 h (Figure 4D). These data point to a key role of the CoREST complex in suppressing Treg production of cytokines that are characteristic of activated conventional T cells and only dysfunctional Treg cells.

Rcor1 deletion disrupts the Hdac/Lsd1/CoREST complex in Tregs. The CoREST complex, whose primary components are Hdac1 or its paralog Hdac2, Lsd1, and the scaffolding protein CoREST/Rcor1, regulates chromatin remodeling and gene expression (14, 26, 27). Upon studying *Rcor1* protein expression in Tregs, we found that *Rcor1* was located in cytoplasm under basal conditions in WT Tregs, but after activation with CD3/CD28 mAbs for 24 hours, *Rcor1* translocated to the nucleus (Figure 5A), consistent with reports that phosphorylation of *Rcor1* in T cells and other cells can lead to nuclear translocation of cytoplasmic *Rcor1* (28, 29). Next, we found that the levels of Hdac2 and Lsd1 proteins, but not that of Hdac1, were significantly decreased in *Rcor1*^{-/-} Tregs (Figure 5B). The best studied modification of core histones is the reversible acetylation of conserved lysine residues within N-terminal tails, as regulated by histone acetyltransferases (Hats) and Hdacs. A well-established feature of CoREST is its ability to regulate H3K9 acetylation and H3K4 demethylation (15-17).

In *Rcor1*^{-/-} Tregs, we found that H3K9 acetylation (H3K9Ac) and H3K4 di-methylation (H3K4Me2) were increased compared to WT Tregs, consistent with reduced actions of the CoREST Hdac and Lsd1 enzymes (Figure 5C). Likewise, overexpression of *Rcor1* in 293T cells decreased the levels of H3K9Ac and H3K4Me2 (Figure 5D). These data indicate that *Rcor1* is important to maintaining CoREST complex-dependent functions in Treg cells.

Rcor1 deletion disrupts Treg function in vivo and promotes anti-tumor immunity. We used three animal models to assess the effects of *Rcor1* deletion on Treg function in vivo (23, 30). First, we tested the ability of Tregs to inhibit homeostatic proliferation of conventional T cells over 7 days following their adoptive transfer into immunodeficient mice. Co-transfer of WT Tregs significantly inhibited Teff cell proliferation, whereas *Rcor1*^{-/-} Tregs were less able to suppress Teff cell proliferation (p<0.05, Figure 6A) and showed upregulation of IFN- γ production (Supplemental Figure 6A). Analogous adoptive transfer with follow-up at 30 days again showed markedly greater expansion of Teff cells in the presence of *Rcor1*^{-/-} vs. WT Tregs, and suggested that decreased viability of YFP⁺ *Rcor1*^{-/-} vs. WT Tregs may contribute to this difference given the reduced number of viable *Rcor1*^{-/-} vs. WT Tregs (Figure 6B). *Rcor1*^{-/-} Tregs also showed increased production of IL-2 and IFN- γ compared to WT Treg cells (Supplemental Figure 6B).

In a second in vivo test of *Rcor1* deletion in Tregs, we undertook cardiac allografts and treated recipients with CD40L (CD154) mAb plus donor splenocyte (5×10^6) transfusion (DST). This well-established costimulation blockade protocol (31) induced long-term allograft survival in WT but not in *Rcor1*^{-/-} recipients (Figure 6C), indicating the inability of Foxp3⁺ Tregs to control host alloresponses in the absence of *Rcor1*.

Third, we assessed whether *Rcor1* deletion in Tregs promoted anti-tumor immunity, using TC1 and AE.17 lung tumor models. We have previously shown that the growth of these tumors in syngeneic C57BL/6 mice is Treg-dependent (23, 32). Compared with WT mice, *Rcor1*^{-/-} mice displayed a profound reduction in AE.17 tumor growth (Figure 6D). Flow cytometry analysis showed that *Rcor1*^{-/-} mice had an increased frequency of tumor-infiltrating IFN- γ -producing CD8⁺ T cells (Figure 6E), and qPCR analysis showed increased CD4, CD8, IFN- γ and granzyme-B mRNAs, and decreased Foxp3 mRNA, in tumors harvested from *Rcor1*^{-/-} vs. WT mice (Figure

6F). Related studies in the TC1 lung tumor model showed that compared to WT controls, *Rcor1*^{-/-} mice had decreased tumor growth (Figure 6G), increased tumor infiltration by IFN- γ ⁺ CD8 T cells (Figure 6H), and increased CD4, CD8, IFN- γ and granzyme-B mRNAs (Figure 6I). Lastly, consistent with Treg dysfunction upon *Rcor1* deletion, *Rcor1*^{-/-} Tregs produced more cytokines (IL-2, IL-4, IFN- γ) than WT Tregs in tumor associated LN and within the tumors themselves (Supplemental Figure 7). Thus, *Rcor1* deletion in Treg cells impairs Treg function and promotes antitumor immunity.

CoREST complex inhibitor impaired murine Treg function. Bifunctional small molecules that jointly inhibit the Hdac and Lsd1 enzymatic activities of the CoREST complex were recently described (33). The structure of JK-2-68 is derived from phenelzine, while that of JKD-1-51 (also known as Corin) is derived from tranylcyproline, and both compounds contain the same zinc binding group that is derived from the HDAC inhibitor MS-275 (Supplemental Figure 8). From a translational perspective, we questioned whether such bifunctional CoREST inhibitors would generate data in WT mice similar to that found upon disruption of the complex in Foxp3⁺ Treg cells by *Rcor1* deletion? Encouragingly, CoREST inhibitors impaired murine Treg suppressive function (Supplemental Figure 9) but did not affect the suppressive function of *Rcor1*^{-/-} Treg cells (Supplemental Figure 10). We next studied gene expression by purified WT Teff and Foxp3⁺ Treg cells that were freshly isolated or stimulated overnight with CD3/CD28 mAb-coated beads in the presence of DMSO or CoREST inhibitor. CoREST inhibitor treatment resulted in increased gene expression of IL-17 and IFN- γ , and decreased gene expression of Foxp3, CTLA4, GITR and TGF- β by Treg cells, as well as increased IL-2, IL-10 and IFN- γ , and decreased GITR and TGF- β expression by conventional T cells (Figure 7A). Treg induction of pro-inflammatory cytokines, upon CoREST inhibitor treatment, was also seen by flow cytometry (Supplemental Figure 11).

We next used two transplant models (34) that are both dependent upon Foxp3⁺ Treg function for long-term allograft survival (>100 d) to screen for effects of CoREST inhibitors on immune responses in vivo. Adoptive transfer of Teff and Treg cells (2:1 ratio) into *Rag1*^{-/-} cardiac allograft recipients led to long-term (>100 d) survival in the case of DMSO-treated mice, but resulted in acute allograft rejection in mice treated with JK-2-68 (10

mg/kg/d, 14 d) ($p < 0.01$) (Figure 7B) or Corin ($p < 0.01$, Supplemental Figure 9D). Likewise, the CD40L mAb-based costimulation blockade protocol resulted in long-term (>100 d) allograft survival in DMSO-treated mice but led to allograft rejection in recipients treated with JK-2-68 ($p < 0.01$) (Figure 7C). We also tested the effects of JK-2-68 on histone acetylation and demethylation in Foxp3⁺ Treg cells and found that the levels of H3K9Ac and H3K4Me2 were markedly increased (Figure 7D). These results indicate that CoREST complex inhibition impairs the functions of murine Treg cells in vitro and in vivo.

CoREST complex inhibitor impaired human Treg function. In parallel studies, preincubation of human Tregs with Corin impaired Treg suppression of the proliferation of human CD4 (Figure 8A) and CD8 (Supplemental Figure 12) T cells. By staining cells harvested at the end of these suppression assays for the fixable live/dead marker Zombie and FOXP3, and gating on CD4⁺CFSE⁻ cells to define “dead Treg” Zombie⁺, “live exTreg” Zombie⁻FOXP3⁻, and “live Treg” Zombie⁻FOXP3⁺ cells, we found that Corin exposure had decreased the numbers of live Tregs and increased the numbers of exTregs in these assays (Figure 8B). Statistical analyzes of these effects are shown in Figure 8C and 8D, respectively. We also noted that Corin had decreased Treg expression of FOXP3 and CTLA4 (Figure 8E) and increased expression of CD127 (Figure 8F). Studies of the direct effects of Corin on human PBMC showed that the compound led to decreased proportions of FOXP3⁺ cells (Figure 8G) and decreased FOXP3 protein expression per Treg cell (Figure 8H), with statistical analyzes in Figure 8I and 8J, respectively. Hence, CoREST inhibitor treatment impaired human Treg suppressive function and was associated with decreased expression of Foxp3, CTLA4 and other genes associated with human Treg function.

CoREST complex inhibitor promotes antitumor immunity. While the murine transplant data suggested that CoREST inhibition preferentially affected the functions of Tregs vs. Teff cells, since the net effect of systemic compound administration was to induce allograft rejection by host T cells, a far more significant action would be to promote antitumor immunity, consistent with the effects we observed following Rcor1 deletion in Foxp3⁺ Treg cells (Figure 6). For these studies, we turned to use of Corin, a more powerful and pharmacokinetically robust CoREST complex inhibitor than JK-2-68 (33). Importantly, like JK-2-68, Corin impaired Treg function in vitro and in vivo (Supplementary Figure 9). Compared to DMSO-treated controls, syngeneic C57BL/6 mice treated with Corin had significantly reduced growth of TC1 tumors (Figure 9A). This beneficial effect was accompanied

by increased tumor infiltration by CD8⁺ T cells (Figure 9B), including CD8⁺IFN- γ ⁺ T cells (Figure 9C). Tumor infiltration by Foxp3⁺ Tregs was unchanged by Corin therapy (Figure 9D) but these cells now produced pro-inflammatory cytokines, including IL-2 and IFN- γ (Supplemental Figure 13). CoREST complex inhibitor therapy also promoted CD4 and CD8 T cell activation in secondary lymphoid tissues, and increased tumor infiltration by effector/memory CD8⁺T cells (Figure 9E). Hence, use of a CoREST complex inhibitor promoted antitumor immunity and thereby impaired tumor growth in WT mice, since no direct effects on tumor growth were seen when tumor-bearing immunodeficient Rag1^{-/-} mice (Supplemental Figure 14).

Discussion

Comparative studies of the three CoREST genes, encoding Rcor1 and its paralogs Rcor2 and Rcor3, indicate that all three CoREST proteins interact equally with Lsd1 but vary in their dependency on Hdac1/2 for their transcriptional repression (35). CoREST complexes containing Rcor1 have the greatest transcriptional repressive capacity (35). In the current studies, pulldown of Foxp3 led to co-immunoprecipitation of Rcor1 but not Rcor2, and pulldown of Lsd1 led to co-immunoprecipitation of Foxp3 only in the presence of Rcor1 (Figure 1). These biochemical data suggest that Rcor1 and Lsd1 are important to Treg biology, consistent with the presence of Foxp3, Rcor1, Hdac1 or Hdac2 and Lsd1, but not Rcor2 or Rcor3, in large multiprotein complexes of 400-800 kDa or more in Treg cells (22). Also consistent with a major role in Tregs of Rcor1 versus its paralogs, Rcor2 deletion had minimal effects on Tregs, and dual Rcor/Rcor2-deficient Tregs were similar to Rcor1^{-/-} Tregs (Supplemental Figure 2). Under basal conditions, deletion of Rcor1 had only modest effects on Treg development and numbers in secondary lymphoid tissues, and Rcor1^{-/-} mice developed normally and had no signs of autoimmunity when housed under specific pathogen-free conditions for up to a year. Upon activation in vitro, Rcor1 deletion or use of CoREST inhibitors promoted Treg production of pro-inflammatory cytokines but in the resting state, tissues were not infiltrated by host cells (Supplemental Figure 15). In contrast, our data from homeostatic proliferation studies, cardiac transplant experiments and tumor models all point to a critical loss of Treg function when Rcor1^{-/-} mice were challenged by strong T cell activation in vivo. The apparent disconnect between minor effects in vitro and in vivo in Rcor1^{-/-} mice under basal conditions compared to when subject to activating stimuli is not unusual. E.g. The ablation of Blimp1, Icos, IL-10, Ctl4 or Eos in Tregs does not impact their suppressive properties in vitro, but impairs their activation under stimulating conditions and their activities in vivo (36-41), similarly to our Rcor1^{-/-} mice. These data and our related findings using bifunctional CoREST inhibitors in WT mice underscore the potential benefit of targeting this complex for therapeutic purposes, such as in cancer immunotherapy.

Deletion of Rcor1 in Tregs increased the expression of multiple transcription factors, cytokines, chemokines, and their receptors, especially upon cell activation (Figure 3). Prominent among these effects were the induction

of IL-2 and IFN- γ production by Rcor1^{-/-} Tregs, consistent with decreased recruitment of Lsd1, Hdac1 and/or Hdac2 to the *Il2*, *Ifng* and *Tbox1* gene promoters and increased histone-3 acetylation at these sites (Figure 4). A key role of the CoREST complex in normally suppressing these events was further supported by the findings of increased H3K4Me2 and H3K9Ac in Rcor1^{-/-} vs. WT Tregs, consistent with decreased actions of Lsd1 and Hdac1/2, respectively, as well as by reversal of these features upon overexpression of Rcor1 (Figure 5). Treg cells are sensitive to changes in the amount of IL-2 produced by CD4⁺Foxp3⁻CD44^{hi} T cells, and this is thought to be a mechanism by which Treg cell abundance can be rapidly altered as the number of Teff cells fluctuates (42). Likewise, Foxp3 binds and prevents the expression of effector cytokine genes in Tregs (43). The disruption of the epigenetic regulation of IL-2, IFN- γ and other genes in Tregs as a result of Rcor1 deletion points to additional levels of control, and potential for therapeutic intervention, beyond regulation of the activation of transcription factors, their DNA binding and recruitment of transcriptional complexes, as shown schematically in Figure 10.

The in vivo effects of Rcor1 deletion in Tregs were more potent than anticipated by our in vitro data but are consistent with a reduced transcriptional repressive capacity compared to WT Tregs, and decreased suppression of potent Teff responses induced by exposure to allogeneic cells and tumor antigens. We have shown that the ability of AE.17 and TC1 tumor cells to grow in syngeneic C57BL/6 mice is dependent upon the ability of Foxp3⁺ Treg to suppress host Teff responses, especially that of CD8⁺ T cells producing effector molecules such as IFN- γ and granzyme-B (23, 32). The findings that deletion of Rcor1 within Tregs of tumor bearing mice had profound effects on tumor growth and immune-dependent clearance points to a major role of the CoREST complex in control of Treg functions during potent immune responses. These events were not accompanied by an inability of Foxp3⁺ Tregs to accumulate at tumors, since flow cytometric studies showed that Treg numbers were unimpaired or even somewhat increased (Figure 6), possibly reflecting increased CXCR3 expression following Rcor1 deletion. Overall, the findings in Rcor1^{-/-} mice are more consistent with disruption of function as a result of derepression of multiple genes within Foxp3⁺ Treg cells than with effects on Treg trafficking or survival at tumor sites.

Encouraged by the *in vivo* data following *Rcor1* targeting in Treg cells, we turned to testing of recently characterized bifunctional CoREST inhibitors (33) in WT mice. These compounds were known to inhibit the proliferation of various tumor lines *in vitro*, as well as having inhibitory effects on the growth of SK-MEL-5 melanoma cell xenografts in immunodeficient mice (33). However, their utility in syngeneic models has not been reported. Since *in vivo* use of these compounds could have effects beyond just Treg cells, we first focused on testing effects of one such CoREST complex inhibitor, JK-2-68, on resting or activated Tregs and conventional T cells. In *Foxp3*⁺ Treg cells, the inhibitor decreased expression of several signature genes, including genes encoding CTLA4, *Foxp3*, GITR and TGF- β , increased IFN- γ and IL-17 expression, and resulted in increased H3K4Me2 and H3K9Ac levels. In conventional T cells, the compound increased IL-2 and IFN- γ production. Hence, the overall brunt of the effects was to dampen Treg genes and promote Th1 responses. However, it should be noted that changes in H3K4Me1/2 - the mark targeted by *Lsd1*, is classically an enhancer rather than a promoter mark, such that the observed effects on gene expression could well be mediated by changes in the enhancer landscape rather than by direct effects at the various gene promoters.

Consistent with its immune activating effects, JK-2-68 therapy in two distinct allograft models in which Treg function is required for long-term transplant survival, resulted in allograft rejection. Lastly, the more powerful and pharmacokinetically robust compound, Corin, also impaired Treg suppressive function, significantly reduced growth of TC1 tumors in syngeneic mice, and was associated with increased host effector responses, including infiltration by activated CD8⁺ T cells producing IFN- γ . While understanding the mechanisms underlying these events is likely more nuanced than studies using conditional deletion of *Rcor1* in Tregs, the transplant data indicate that the brunt of the effects of JK-2-68 or corin therapy were on the Tregs more than conventional T cells, given that the compound induced acute rejection in Treg-dependent models. Likewise, the cellular and molecular events in Treg-dependent tumor models in *Rcor1*^{-/-} mice and inhibitor-treated mice have many similarities. In conclusion, while further studies of the roles of *Rcor2* and *Rcor3* in Tregs and immune responses generally are warranted, the current work shows that *Rcor1* and the CoREST complex have important roles in *Foxp3*⁺ Tregs, such that therapeutic manipulation using CoREST complex inhibitors may of benefit in cancer immunotherapy.

Methods

Mice. We used WT BALB/c and WT C57BL/6, Rag1^{-/-} C57BL/6, CD90.1/B6 mice, Rcor1^{fllox/fllox} (#025877) and Rcor2^{fllox/fllox} (#030004) from The Jackson Laboratory, plus previously described Foxp3^{YFP-cre} mice (38). All mice were backcrossed on the C57BL/6 background at least 8 times and used at 6–8 weeks of age unless specified.

Plasmids and CoREST complex inhibitors. We purchased plasmids from Addgene and transiently expressed Flag-myc-tagged-Rcor1, Flag-myc-tagged-Rcor2, Flag-tagged-Foxp3 and HA-tagged-p300 in 293T cells (23). Preparation of CoREST complex inhibitors JK-2-68 and JKD-1-51 (corin) was described previously (33).

Co-immunoprecipitation (Co-IP) and Western blotting. HEK-293T cells transfected with plasmids, as well as WT and Rcor1^{-/-} Tregs, were lysed with RIPA buffer (Sigma, #SLBL7395V). Pull-down antibody was incubated with pre-cleared samples for 2 hours at 4 °C, then overnight with Protein-G agarose (Invitrogen, #15920-010). Cell lysates were separated by SDS-PAGE, transferred to PVDF membranes and immunoblotted with the indicated Abs. We purchased Abs against Rcor1 (Millipore, #MABN486), Foxp3 (Invitrogen, #700914, eBioscience, #14-4774-82) and Histone-H3 (Abcam, #ab1791), as well as Flag (#14793), Myc (#2272), HA (#2367), Rcor2 (#ab37113), Lsd1 (#2139), β -actin (#3700), Hdac1 (#34589), Hdac2 (#57156), Pcaf (#3378), T-bet (#13232), β -catenin (#8480), H3K9ac (#9649), H3K4me2 (#9725), ac-Histone-3 (#9754S) from Cell Signaling Technology. Secondary HRP-conjugated Abs to mouse (#7076), rat (#7077) and rabbit (#7074) IgG were purchased from CST. Unconjugated CD3 (clone 145-2C11, #553057) and CD28 (clone 37.51, #553294) mAbs used for cell activation were purchased from BD.

Flow cytometry. Single-cell suspensions from lymph nodes, spleens or tumors were prepared as previously described (33) and were stained with fluorochrome-conjugated mAbs from BD Biosciences, unless specified otherwise, that were directed against CD4 (Pacific blue, Invitrogen, #MHCD0428), CD8 (Super Bright 645, eBioscience, clone 53-6.7, #64-0081-82), Foxp3 (eFluor 450, eBioscience, clone FJK-16s, #48-5773-82), CD62L (PE-Cy7, clone MEL-14, #25-0621-82), IFN- γ (APC, clone XMG1.2, #554413), CD44 (PE-Cyane5, eBioscience, clone IM7, #15-0441-83), and CD25 (APC, eBioscience, clone PC61.5, #17-0251-82) and acquired on a Cytotflex (Beckman Coulter) flow cytometer.

Murine Treg suppression assays. For in vitro studies, 5×10^4 cell-sorted CD4⁺CD25⁻ T cells and CD4⁺CD25⁺ Tregs from Foxp3^{YFP-Cre} and Rcor1^{-/-} mice isolated using CD4⁺CD25⁺ Treg isolation kit (Miltenyi Biotec, #130-091-041) were added to 96-well plates. Equal numbers of CFSE-labeled CD4⁺CD25⁻ T cells and γ -irradiated antigen-presenting cells (APC), isolated using a CD90.2 kit (Miltenyi Biotec, #130-049-101), plus CD3 ϵ mAb (1 μ g/ml), were cultured for 72 h. After 72 h, proliferation of Teff cells was determined by flow and analysis of cell trace violet dilution. For in vivo Treg suppression assays, 1×10^6 CD4⁺CD25⁻ Thy1.1⁺ and 0.5×10^6 Tregs were injected i.v. into Rag1^{-/-} mice. At 1 week, lymph node and spleen cells were stained with Thy1.1-PE and CD4-Pacific blue, and the numbers of Thy1.1⁺ T cell cells determined (Cytotflex).

Corin and human Tregs. Human Treg suppression assays, using Tregs and Teff cells isolated from the peripheral blood of healthy donors, were performed as described (44). Human Treg were pre-incubated for 2.5 hours with Corin (1 μ M), washed two times and used in suppression assays with CFSE-labeled healthy donor PBMC responder cells, stimulated with anti-CD3 ϵ microbeads, for 5-6 days. The ability of Tregs to suppress divisions of CD4⁺ and CD8⁺ T cell responders was analyzed separately. Five independent experiments were performed using 5 different healthy donors of normal Tregs and 3 different healthy donor responders, and most assays used pre-treatment of Tregs with 1 μ M of Corin, such that data from 12 suppression assays were collected.

In addition, we assessed the effects of Corin on human PBMC. PBMC from 5 healthy donors were incubated overnight with Corin (1 μ M) and CD3 ϵ /CD28 mAb-coated beads (1.3 beads/cell) and analyzed the next day by flow cytometry. In total, 18 markers were evaluated in CD45⁺Ghost⁻CD4⁺FOXP3⁺ Treg (IFN- γ , IL-2, IL-4, IL-17, CD45RA, CD45RO, CD62L, CD69, PTEN, CD39, FAS, CD120b, GITR, TIGIT, CD127, CTLA4, HLA-DR, CD25). For cytokine production, PBMC were stimulated the next day for 4 hours with PMA/ionomycin in the presence of Brefeldin. Human healthy donor Tregs did not produce substantial amounts of cytokines, so we noted only the markers whose expression was altered by the presence of Corin.

Cardiac transplantation. Heterotopic cardiac allografts were performed using BALB/c donors and WT or Rag1^{-/-} recipients (C57BL/6 background), as described (30). In adoptive transfer studies of Treg-dependent allograft survival, after their isolation using magnetic beads, Tregs (0.5×10^6) from WT or Rcor1^{-/-} mice, and T

effector cells (1×10^6) from WT mice, were injected i.v. into Rag1^{-/-} mice bearing BALB/c cardiac allografts. In studies of costimulation blockade-dependent allograft tolerance, WT or Rcor1^{-/-} allograft recipients were treated at the time of engraftment with CD154 mAb plus 5×10^6 donor splenocytes (31). Graft survival was monitored as a function of the ability of Tregs to suppress Teff cell-dependent alloreactivity and cardiac allograft rejection. In related pharmacologic studies, Rag1^{-/-} allograft recipients receiving adoptive transfer, or WT recipients treated with CD154 mAb, respectively, were treated with CoREST inhibitors (10 mg/kg/d, 14 d) from engraftment.

ChIP assays. We purchased EZ-Magna ChIP A Chromatin Immunoprecipitation kits (Millipore). Teffs or Tregs were fixed with 1% formaldehyde and fragmented by sonication. Chromatin was immunoprecipitated with Abs against acetyl-Histone-H3, Hdac1, Hdac2 and Lsd1, and the resultant DNA was purified and analyzed by real-time PCR (Step-One, Applied Biosystems). *Il2* and *Ifng* primer sets were reported previously (45); primers for *Tbox1* were forward: CGAATTCGCGCTGTATTAGCC and reverse: GGCCTTTGCTGTGGCTTTAT.

RNA-seq and real-time qPCR. RNA was isolated using RNeasy kits (QIAGEN), and RNA integrity and quantity were analyzed by NanoDrop ND-1000 and Nanochip 2100 Bioanalyzer (Agilent Technologies). Library preparation and RNA sequencing, genome mapping and analysis were performed by Novogene (Sacramento, CA) on the Illumina Platform PE150; data were deposited at the NCBI GEO site (accession GSE137137). Data were tested for differential expression significant analysis using the DESeq2 R package with the significant criterion of a false-discovery rate adjusted p-value (padj) of <0.05, and further analyzed by Gene Ontology, KEGG and Reactome database enrichments. To show z-scores, we have included the three replicates per conditions, and calculated z-score values via the formula: $z = (x - \mu) / \sigma$, with x representing the fragments per kilobase million value, μ representing the mean per row (gene), and σ representing the standard deviation per row (gene). We then generated heat maps using the Morpheus app on the Broad Institute's website (<https://software.broadinstitute.org/morpheus/>). Expression of individual genes was verified by qPCR. RNA was reverse transcribed to cDNA (Applied Biosystems) and qPCR performed using Taqman primer and probe sets; data were normalized to endogenous 18s rRNA, and relative expression was determined by the formula $2^{-\Delta CT}$.

Immunofluorescence. Cell cytopspins were fixed, permeabilized with 0.2% Triton-100, blocked with normal goat serum for 1 hour, incubated with Abs to Foxp3 (rat anti-mouse eBioscience, #14-5773-82), and Rcor1

(mouse anti-mouse, Millipore, #MABN486) diluted in 0.2% Triton-X100 overnight. After washing, cytopspins were incubated with Alexa Fluor 488 conjugated goat anti-rat IgG (Invitrogen A11006) and Alexa Fluor 594 conjugated goat anti-mouse IgG (Invitrogen A11032), nuclei were stained with Hoechst (1 ug/ml, CST 4082), and cells were analyzed by fluorescent microscopy.

Cell lines and tumor model. TC1 cells, derived from mouse lung epithelial cells that were immortalized with HPV-16 E6 and E7, and transformed with the c-Ha-ras oncogene (46), were provided by Dr. Yvonne Paterson (UPenn, Philadelphia, PA). The murine AE17.ova mesothelioma cell line (provided by Dr. Delia Nelson, University of Western Australia, Perth, Australia) was derived from mesothelioma cells developing in mice treated i.p. with asbestos, and then stably transduced with chicken ovalbumin (47). Cells were grown in RPMI, 10% fetal bovine serum (FBS), 2 mM glutamine, and 5 µg/ml of penicillin and streptomycin. Each mouse was shaved on their right flank and injected s.c. with 1.2×10^6 TC1 or 2×10^6 AE17 tumor cells. Tumor volume was determined by the formula: $(3.14 \times \text{long axis} \times \text{short axis} \times \text{short axis})/6$.

Statistics. Data were analyzed using GraphPad Prism8.0. Data are presented as mean \pm SD unless specified otherwise. Measurements between two groups were done with a 2-tailed Student's t test if data were normally distributed or Mann-Whitney U unpaired test when the populations were not normally distributed. Groups of 3 or more were analyzed by 1-way ANOVA with corresponding Tukey's multiple comparison test if normally distributed, or if not, using the Kruskal-Wallis with Dunn's multiple comparison test. Graft survival was evaluated with Kaplan-Meier followed by log-rank test; $p < 0.05$ was considered significant. For human Treg suppression assays, AUC were calculated as described (44), followed by calculation of the ratios of AUCs to control Treg AUCs. For data presented as ratios, one sample T test (theoretical mean = 1) was applied for normally distributed data, otherwise we applied Wilcoxon Signed rank test (theoretical median = 1). When needed, all p values were corrected with Bonferoni test for multiple comparisons. FOXP3 MOF (median of fluorescence) data were calculated using unpaired Student's t-test.

Study approval. Animal studies were approved by the Institutional Animal Care and Use Committee of the Children's Hospital of Philadelphia (protocols 17-001047 and 19-000561).

Author contributions

Y.X. designed and performed experiments and drafted the manuscript. L.W. performed cardiac transplants and performed experiments. R.H. provided technical assistance. E.D.G. performed experiments. U.H.B. provided assistance with RNA-seq studies. T.A. performed studies. M.T. performed studies. J.K. provided assistance with CoREST complex inhibitors. P.A.C provided assistance with CoREST complex inhibitors and assistance with the manuscript. W.W.H. oversaw experimental design and writing of the manuscript.

Acknowledgments

This work was supported by NIH grants R01 AI12324 and R01 CA177852 (to W.W. Hancock), as well as R37GM62437 (to P.A. Cole), and specified plasmids were purchased from Addgene.

References

1. Sakaguchi S, Yamaguchi T, Nomura T, and Ono M. Regulatory T cells and immune tolerance. *Cell*. 2008;133(5):775-87.
2. Josefowicz SZ, Lu LF, and Rudensky AY. Regulatory T cells: mechanisms of differentiation and function. *Annu Rev Immunol*. 2012;30:531-64.
3. Bauer CA, Kim EY, Marangoni F, Carrizosa E, Claudio NM, and Mempel TR. Dynamic Treg interactions with intratumoral APCs promote local CTL dysfunction. *J Clin Invest*. 2014;124(6):2425-40.
4. Fontenot JD, Gavin MA, and Rudensky AY. Foxp3 programs the development and function of CD4⁺CD25⁺ regulatory T cells. *Nat Immunol*. 2003;4(4):330-6.
5. Hori S, Nomura T, and Sakaguchi S. Control of regulatory T cell development by the transcription factor Foxp3. *Science*. 2003;299(5609):1057-61.
6. Van Gool F, et al. A mutation in the transcription factor Foxp3 drives T helper 2 effector function in regulatory T cells. *Immunity*. 2019;50(2):362-77 e6.
7. Miguel A, et al. Silencing of Foxp3 enhances the antitumor efficacy of GM-CSF genetically modified tumor cell vaccine against B16 melanoma. *Oncotargets and therapy*. 2017;10:503-14.
8. Sakaguchi S, Sakaguchi N, Asano M, Itoh M, and Toda M. Immunologic self-tolerance maintained by activated T cells expressing IL-2 receptor alpha-chains (CD25). Breakdown of a single mechanism of self-tolerance causes various autoimmune diseases. *J Immunol*. 1995;155(3):1151-64.
9. Wang L, et al. Foxp3⁺ T-regulatory cells require DNA methyltransferase 1 expression to prevent development of lethal autoimmunity. *Blood*. 2013;121(18):3631-9.

10. Sharma A, et al. Anti-CTLA-4 immunotherapy does not deplete FOXP3(+) regulatory T cells (Tregs) in human cancers. *Clin Cancer Res.* 2019;25(4):1233-8.
11. Liu J, and Cao X. Cellular and molecular regulation of innate inflammatory responses. *Cell Mol Immunol.* 2016;13(6):711-21.
12. Andres ME, et al. CoREST: a functional corepressor required for regulation of neural-specific gene expression. *Proc Natl Acad Sci U S A.* 1999;96(17):9873-8.
13. Humphrey GW, et al. Stable histone deacetylase complexes distinguished by the presence of SANT domain proteins CoREST/kiaa0071 and Mta-L1. *J Biol Chem.* 2001;276(9):6817-24.
14. You A, Tong JK, Grozinger CM, and Schreiber SL. CoREST is an integral component of the CoREST-human histone deacetylase complex. *Proc Natl Acad Sci U S A.* 2001;98(4):1454-8.
15. Hakimi MA, Bochar DA, Chenoweth J, Lane WS, Mandel G, and Shiekhattar R. A core-BRAF35 complex containing histone deacetylase mediates repression of neuronal-specific genes. *Proc Natl Acad Sci U S A.* 2002;99(11):7420-5.
16. Yang M, et al. Structural basis for CoREST-dependent demethylation of nucleosomes by the human LSD1 histone demethylase. *Mol Cell.* 2006;23(3):377-87.
17. Lee MG, Wynder C, Cooch N, and Shiekhattar R. An essential role for CoREST in nucleosomal histone 3 lysine 4 demethylation. *Nature.* 2005;437(7057):432-5.
18. Shi Y, et al. Histone demethylation mediated by the nuclear amine oxidase homolog LSD1. *Cell.* 2004;119(7):941-53.
19. Chan FC, et al. An RCOR1 loss-associated gene expression signature identifies a prognostically significant DLBCL subgroup. *Blood.* 2015;125(6):959-66.

20. Monaghan CE, et al. REST corepressors RCOR1 and RCOR2 and the repressor INSM1 regulate the proliferation-differentiation balance in the developing brain. *Proc Natl Acad Sci U S A*. 2017;114(3):E406-E15.
21. Yao H, Goldman DC, Fan G, Mandel G, and Fleming WH. The corepressor Rcor1 Is essential for normal myeloerythroid lineage differentiation. *Stem Cells*. 2015;33(11):3304-14.
22. Rudra D, et al. Transcription factor Foxp3 and its protein partners form a complex regulatory network. *Nat Immunol*. 2012;13(10):1010-9.
23. Liu Y, et al. Inhibition of p300 impairs Foxp3+ T regulatory cell function and promotes antitumor immunity. *Nat Med*. 2013;19(9):1173-7.
24. Hu X, and Ivashkiv LB. Cross-regulation of signaling pathways by interferon-gamma: implications for immune responses and autoimmune diseases. *Immunity*. 2009;31(4):539-50.
25. Sumida T, et al. Activated beta-catenin in Foxp3(+) regulatory T cells links inflammatory environments to autoimmunity. *Nat Immunol*. 2018;19(12):1391-402.
26. Laugesen A, and Helin K. Chromatin repressive complexes in stem cells, development, and cancer. *Cell stem cell*. 2014;14(6):735-51.
27. Mohammad HP, et al. A DNA hypomethylation signature predicts antitumor activity of LSD1 inhibitors in SCLC. *Cancer Cell*. 2015;28(1):57-69.
28. Gu H, Liang Y, Mandel G, and Roizman B. Components of the REST/CoREST/histone deacetylase repressor complex are disrupted, modified, and translocated in HSV-1-infected cells. *Proc Natl Acad Sci U S A*. 2005;102(21):7571-6.

29. Gu H, and Roizman B. Herpes simplex virus-infected cell protein 0 blocks the silencing of viral DNA by dissociating histone deacetylases from the CoREST-REST complex. *Proc Natl Acad Sci U S A*. 2007;104(43):17134-9.
30. Wang L, et al. FOXP3+ regulatory T cell development and function require histone/protein deacetylase 3. *J Clin Invest*. 2015;125(3):1111-23.
31. Hancock WW, Sayegh MH, Zheng XG, Peach R, Linsley PS, and Turka LA. Costimulatory function and expression of CD40 ligand, CD80, and CD86 in vascularized murine cardiac allograft rejection. *Proc Natl Acad Sci U S A*. 1996;93(24):13967-72.
32. Wang L, et al. Ubiquitin-specific protease-7 inhibition impairs Tip60-dependent Foxp3+ T-regulatory cell function and promotes antitumor immunity. *EBioMedicine*. 2016;13:99-112.
33. Kalin JH, et al. Targeting the CoREST complex with dual histone deacetylase and demethylase inhibitors. *Nat Commun*. 2018;9(1):53.
34. Tao R, et al. Deacetylase inhibition promotes the generation and function of regulatory T cells. *Nat Med*. 2007;13(11):1299-307.
35. Barrios AP, et al. Differential properties of transcriptional complexes formed by the CoREST family. *Mol Cell Biol*. 2014;34(14):2760-70.
36. Bankoti R, et al. Differential regulation of effector and regulatory T cell function by Blimp1. *Scientific reports*. 2017;7(1):12078.
37. Guo F, Iclozan C, Suh WK, Anasetti C, and Yu XZ. CD28 controls differentiation of regulatory T cells from naive CD4 T cells. *J Immunol*. 2008;181(4):2285-91.
38. Rubtsov YP, et al. Regulatory T cell-derived interleukin-10 limits inflammation at environmental interfaces. *Immunity*. 2008;28(4):546-58.

39. Sojka DK, Hughson A, and Fowell DJ. CTLA-4 is required by CD4+CD25+ Treg to control CD4+ T-cell lymphopenia-induced proliferation. *Eur J Immunol*. 2009;39(6):1544-51.
40. Paterson AM, et al. Deletion of CTLA-4 on regulatory T cells during adulthood leads to resistance to autoimmunity. *J Exp Med*. 2015;212(10):1603-21.
41. Gokhale AS, Gangaplara A, Lopez-Occasio M, Thornton AM, and Shevach EM. Selective deletion of Eos (Ikzf4) in T-regulatory cells leads to loss of suppressive function and development of systemic autoimmunity. *J Autoimmun*. 2019;105:102300.
42. Setoguchi R, Hori S, Takahashi T, and Sakaguchi S. Homeostatic maintenance of natural Foxp3(+) CD25(+) CD4(+) regulatory T cells by interleukin (IL)-2 and induction of autoimmune disease by IL-2 neutralization. *J Exp Med*. 2005;201(5):723-35.
43. Ono M, et al. Foxp3 controls regulatory T-cell function by interacting with AML1/Runx1. *Nature*. 2007;446(7136):685-9.
44. Akimova T, Levine MH, Beier UH, and Hancock WW. Standardization, evaluation, and area-under-curve analysis of human and murine Treg suppressive function. *Methods Mol Biol*. 2016;1371:43-78.
45. Northrop JK, Thomas RM, Wells AD, and Shen H. Epigenetic remodeling of the IL-2 and IFN-gamma loci in memory CD8 T cells is influenced by CD4 T cells. *J Immunol*. 2006;177(2):1062-9.
46. Lin KY, et al. Treatment of established tumors with a novel vaccine that enhances major histocompatibility class II presentation of tumor antigen. *Cancer Res*. 1996;56(1):21-6.
47. Jackaman C, et al. IL-2 intratumoral immunotherapy enhances CD8+ T cells that mediate destruction of tumor cells and tumor-associated vasculature: a novel mechanism for IL-2. *J Immunol*. 2003;171(10):5051-63.

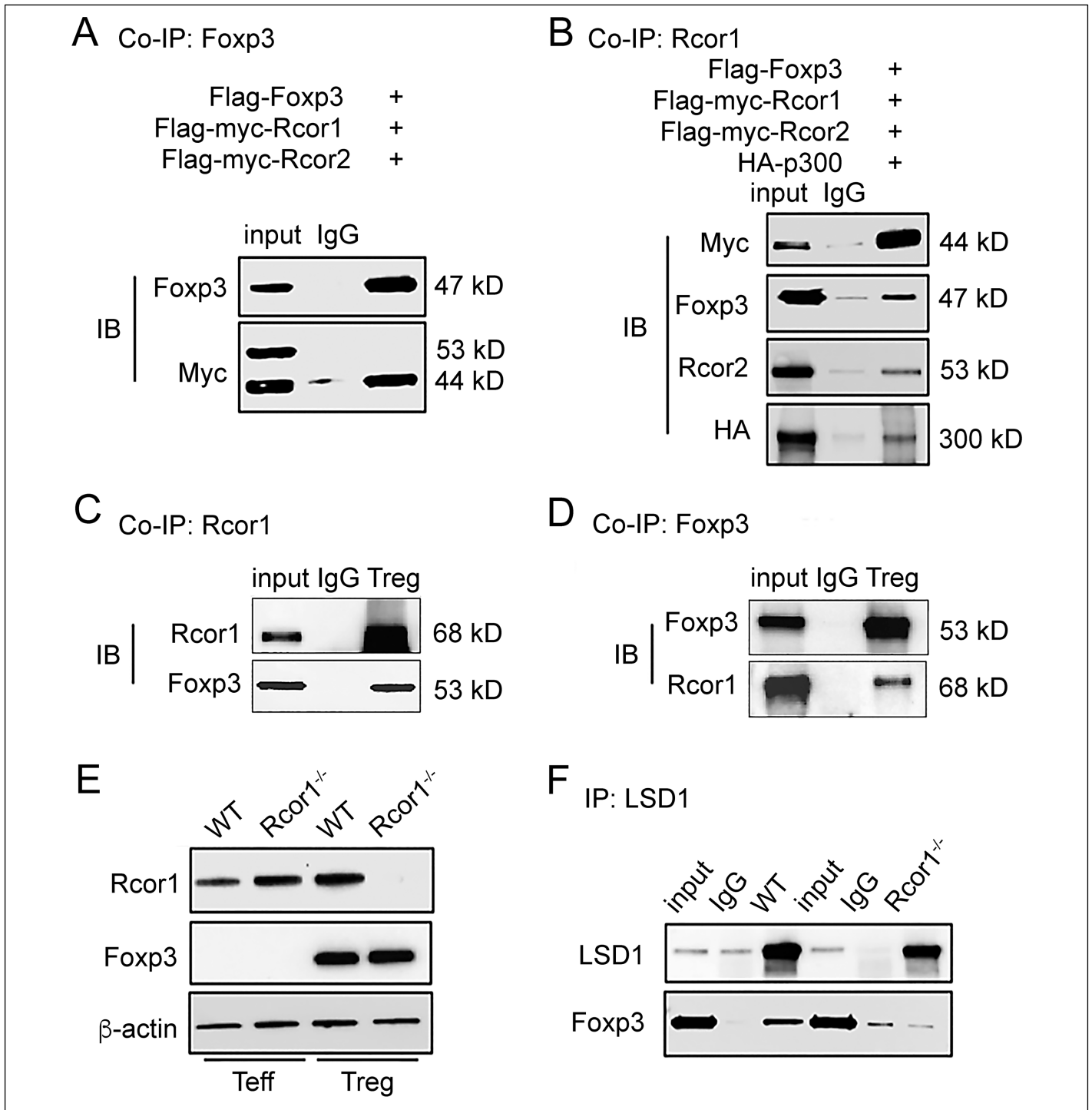
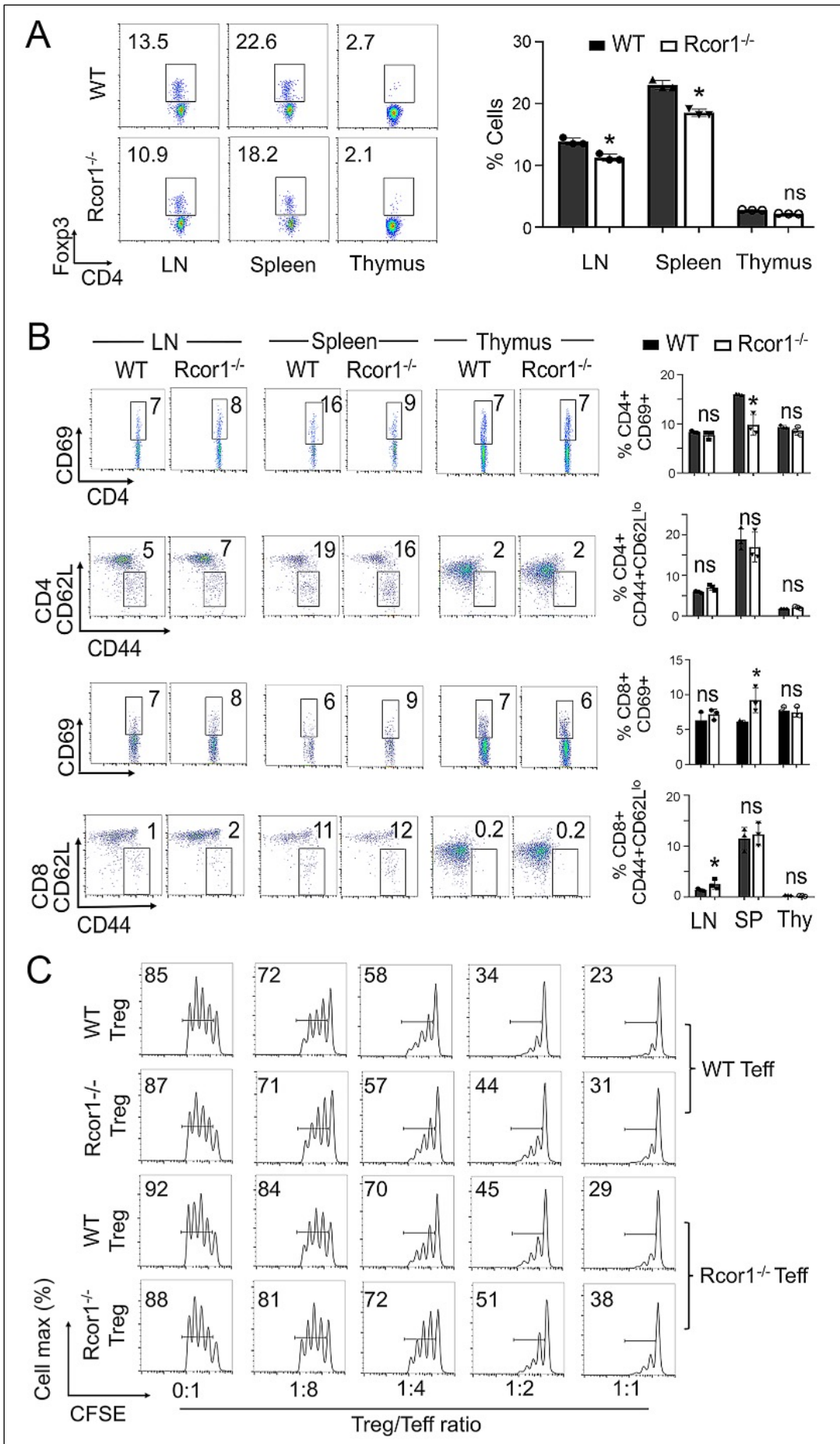


Figure 1. Association of Foxp3 with the CoREST complex. (A) In HEK-293T cells transfected with tagged constructs encoding Foxp3 (47 kD), Rcor1 (44 kD) and Rcor2 (53 kD), immunoprecipitation (IP) of Foxp3 led to co-IP of Rcor1 but not Rcor2 protein. (B) In HEK-293T cells transfected with the same Foxp3, Rcor1 and Rcor2 constructs as used in panel A, plus HA-tagged p300, IP of Rcor1 led to co-IP of Foxp3, Rcor2 and p300. (C) Lysates of Tregs isolated from lymph nodes and spleens of WT B6 mice were subjected to IP using anti-Rcor1 antibody or control IgG; Rcor1 and Rcor1-associated Foxp3 were detected by immunoblotting (IB). (D) Tregs isolated from B6 lymph nodes and spleens after expansion in vivo (rIL-2/anti-IL-2, 3 d), were subjected to IP using anti-Foxp3 Ab or control IgG; panel shows IB detection of Foxp3 and Foxp3-associated Rcor1. (E) Western blots of Rcor1 and Foxp3 expression in Treg and Teff cells from WT mice or those with conditional deletion of Rcor1 in their Tregs; β-actin was used as a loading control. (F) IP of Lsd1 from WT Tregs led to co-IP of Foxp3, whereas IP of Lsd1 from Rcor1^{-/-} Tregs led to only trace levels of Foxp3 co-IP.

Figure 2. Cellular effects of Rcor1 deletion in Foxp3+ Treg cells. (A) Percentages of CD4⁺Foxp3⁺ Tregs in lymph nodes, spleens and thymii of WT and Rcor1^{-/-} mice, shown as representative plots (left) and with statistical analyses (right). (B) T cell activation makers in CD4 and CD8 T cells of WT and Rcor1^{-/-} mice were analyzed as % of gated cells; data shown as representative of 4-6 experiments (left) and with statistical analyses (right). In (E) and (F) data are shown as mean ± SD, 6-8 mice/group, Student's *t* test for unpaired data; **p*<0.05 vs. WT control. (C) Treg suppression assay using pooled (4 mice/group) Tregs from lymph nodes and spleens of WT and Rcor1^{-/-} mice, with representative data shown in G, along with the percentage of proliferating cells in each panel. An experiment was run in triplicate and repeated at least 3 times, and the results of a representative experiment are shown.



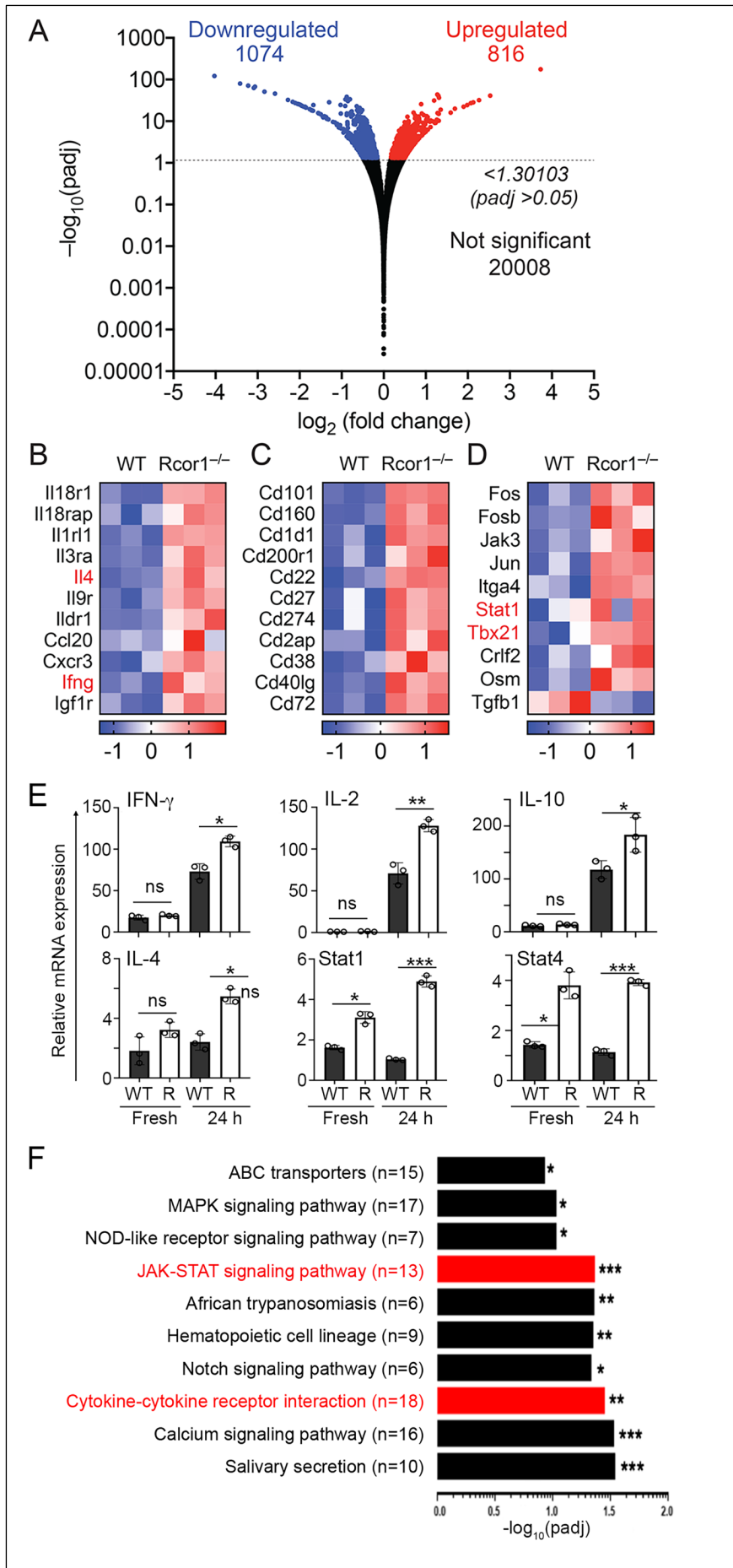


Figure 3. RNA-seq of *Rcor1*^{-/-} vs. WT Tregs. (A) Volcano plot showing statistical significance (false-discovery rate adjusted P value, padj) vs. fold change for genes differentially expressed as a result of *Rcor1* deletion in Foxp3⁺ Treg cells. (B-D) Heatmaps of fragments per kilobase of transcript per million mapped reads of (B) cytokines and cytokine receptors, (C) leukocyte antigens, and (D) transcription factors in WT vs. *Rcor1*^{-/-} Tregs. Data underwent z-score normalization for display. (E) qPCR results of gene expression in WT vs. *Rcor1*^{-/-} (R) Tregs that were freshly isolated or cultured under activating conditions for 24 h (1:1 ratio of CD3/CD28 mAb-coated beads); data are shown as mean \pm SD, 3 mice/group, Student's t test for unpaired data, *P<0.05, **P<0.01, ***P<0.001 for the indicated comparisons. (F) Functional annotation clustering showed enrichment of genes associated with inflammatory and immune responses in *Rcor1*^{-/-} versus WT Tregs.

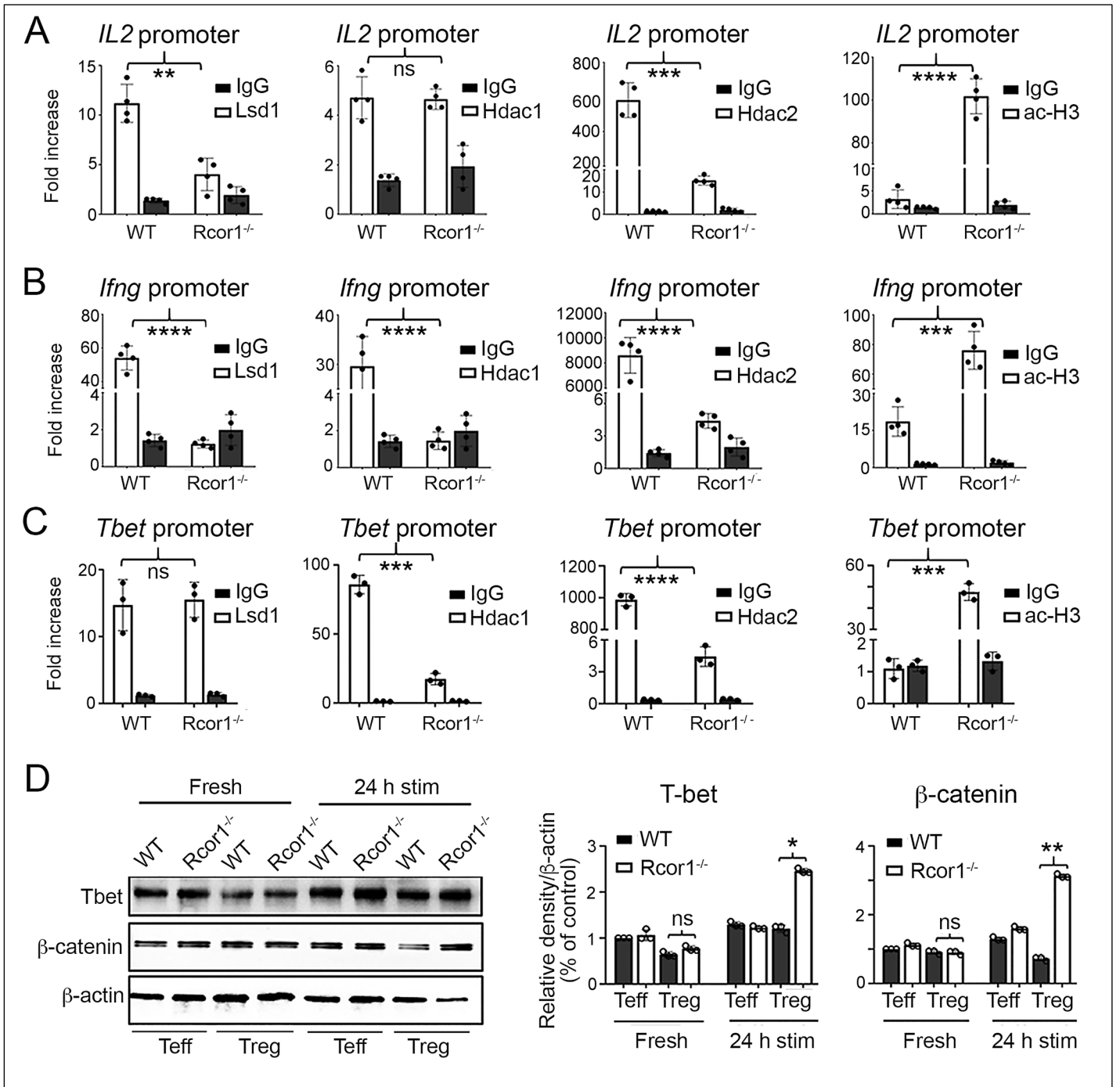


Figure 4. *Rcor1* deletion promotes Treg expression of IL-2, IFN- γ and T-bet. ChIP assays of (A) *Il2*, (B) *Ifng* and (C) *Tbet* promoters with pull-down antibody of Lsd1, Hdac1, Hdac2 and acetyl-Histone 3 (ac-H3). (D) Representative bands and statistical analyses of Western blots for T-bet and β -catenin expression in fresh and 24 hour-stimulated (1:1 ratio of CD3/CD28 mAb-coated beads) WT or *Rcor1*^{-/-} Tregs and Teff cells harvested from corresponding mice. Data are shown as mean \pm SD, 4-6 samples/group, with Student's t-test for unpaired data; * $P < 0.05$, ** $P < 0.01$, *** $P < 0.001$, and **** $P < 0.0001$ vs. WT control.

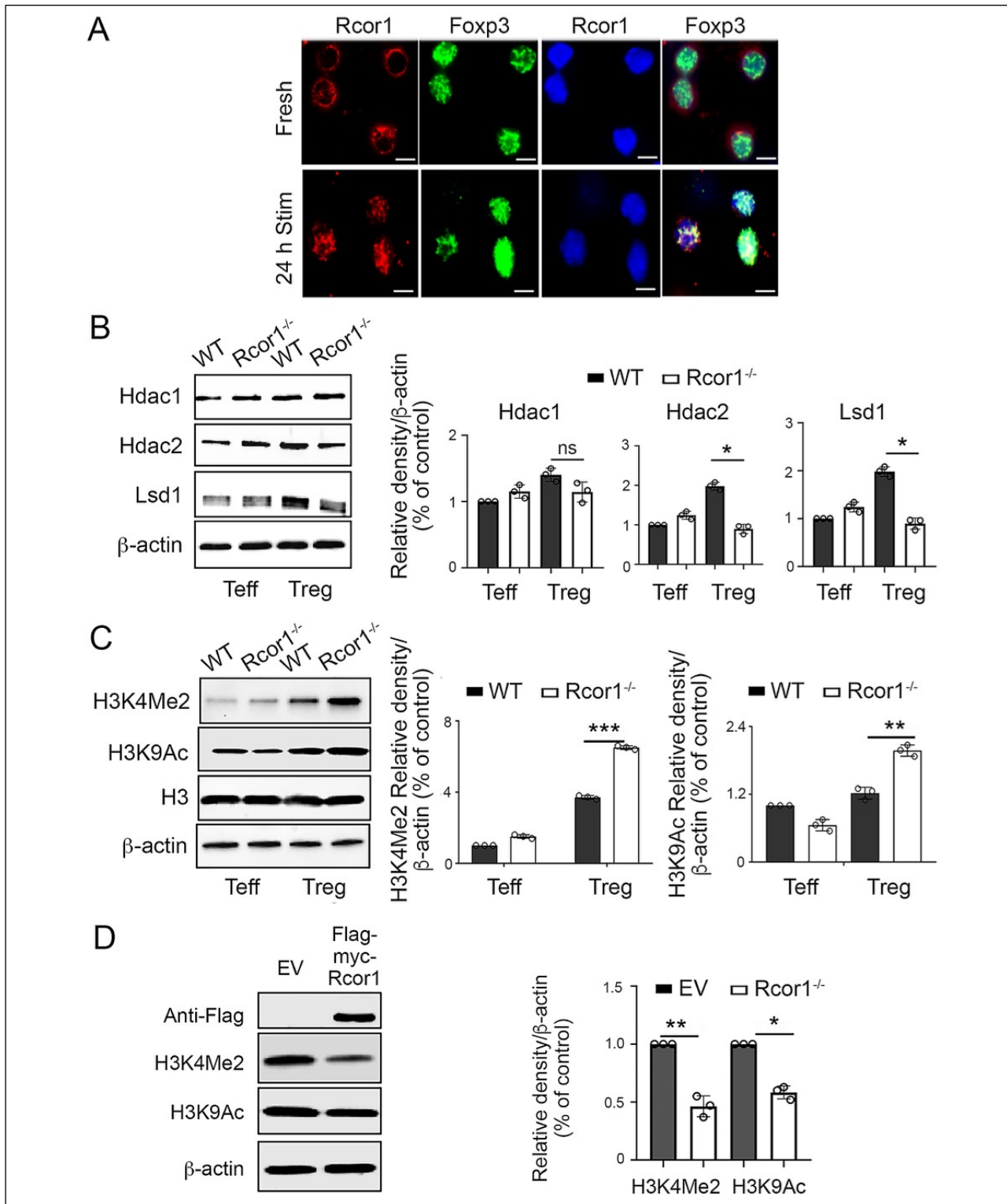


Figure 5. Rcor1 deletion affects the functions of the CoREST complex in Tregs. (A) Localization of Rcor1 and Foxp3 in Tregs (original magnification, 400 \times , representative of 3 independent experiments); scale bar: 10 μ m. (B) Representative bands (left) and statistical analysis (Right) of Western blotting for HDAC1/2/LSD1 in Rcor1^{-/-} versus WT Treg (β -actin loading control). (C) Western blot of H3K4Me2 and H3K9Ac level in Rcor1^{-/-} versus WT Treg (total Histone3 as loading control) (left), and statistical analysis of Western blotting (Right). (D) Western blots result of H3K4Me2 and H3K9Ac level in 293T cell line after overexpression of Rcor1 compared to EV (β -actin loading control) (left), and statistical analysis of Western blotting (right). Data are shown as mean \pm SD, 4-6 samples/group. Student's t-test for unpaired data; *P < 0.05, **P < 0.01, and ***P < 0.001 vs. WT control.

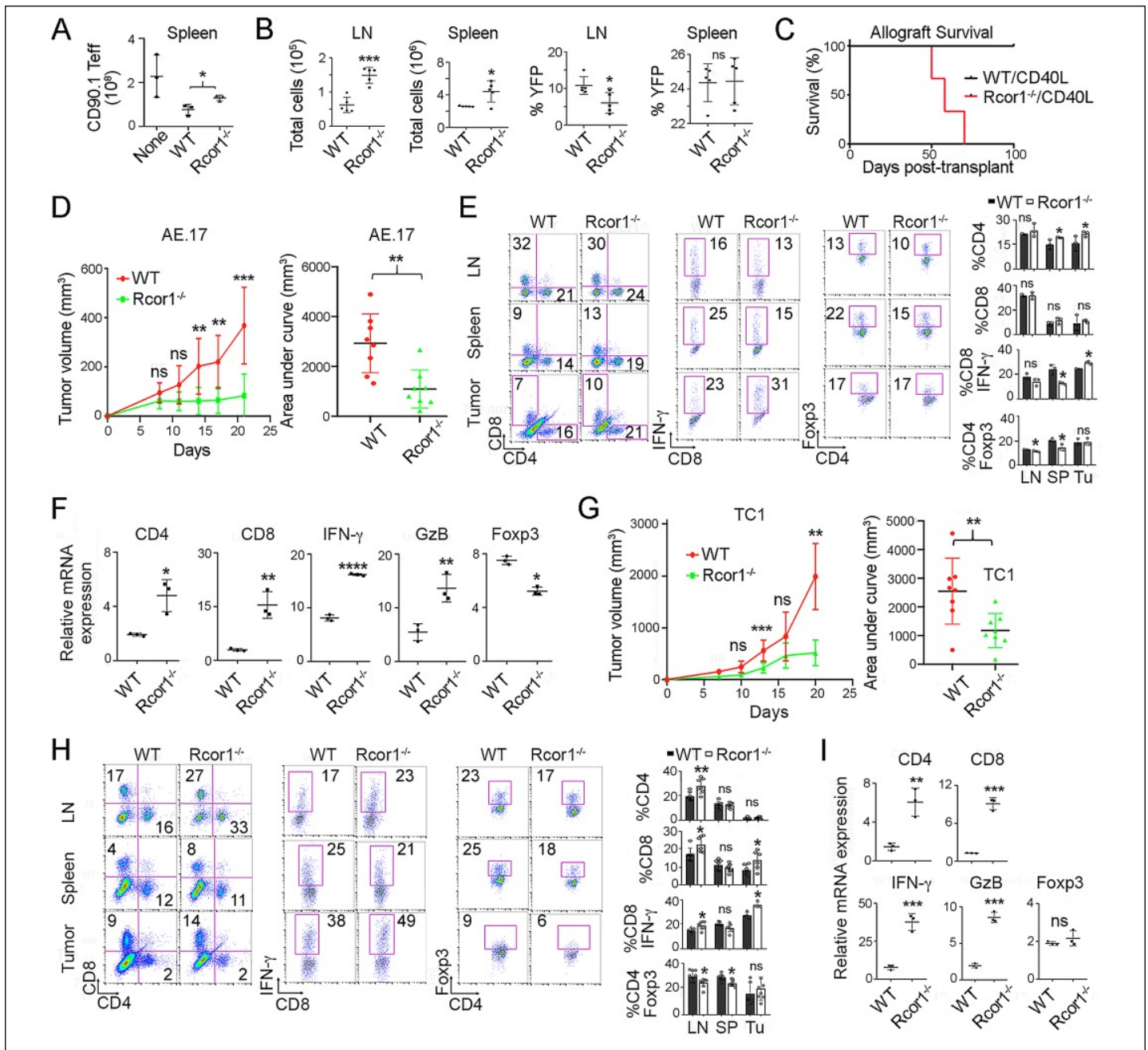


Figure 6. *Rcor1* deletion impairs Treg function in vivo. (A) The ability of *Rcor1*^{-/-} Tregs (0.5×10^6) to dampen homeostatic proliferation at 7 d post-adoptive transfer of Teffs (1×10^6) into *Rag1*^{-/-} mice was significantly decreased compared to the effects of corresponding numbers of WT Tregs ($p < 0.05$). (B) The stability of YFP⁺ *Rcor1*^{-/-} Tregs (1×10^6) at 4 weeks post-adoptive transfer of Teffs (0.25×10^6) in *Rag1*^{-/-} mice was significantly decreased compared to the effects of corresponding WT Treg ($*p < 0.05$, $***p < 0.001$), as shown by flow cytometric evaluation of viable cells. (C) WT or *Rcor1*^{-/-} mice (5 mice/group) received BALB/c cardiac allografts plus CD40L mAb/DST; long-term allograft survival was seen in WT but not *Rcor1*^{-/-} recipients ($p < 0.01$). (D-I) Treg-specific deletion of *Rcor1* enhanced anti-tumor immunity. Tumor volumes and area-under-curve data of AE17 (D) and TC1 (G) lung tumors were smaller in syngeneic *Rcor1*^{-/-} vs. WT mice ($n = 8-10$ /group) after inoculation and reached statistical significance ($*p < 0.05$). Analysis of CD4⁺Fcpx3⁺, CD4⁺, CD8⁺, CD8⁺IFN- γ ⁺ cells in lymphoid tissues from *Rcor1*^{-/-} or WT mice, bearing AE17 (E) or TC1 (H) tumors. qPCR analysis of gene expression of CD4, CD8, IFN- γ , granzyme B and Fcpx3 in tumor samples of AE17 (F) or TC1 (I) harvested at the end of each experiment. Data are shown as mean \pm SD, 4-6 samples/group. Student's t-test for unpaired data; $*P < 0.05$, $**P < 0.01$, and $***P < 0.001$ vs. WT control.

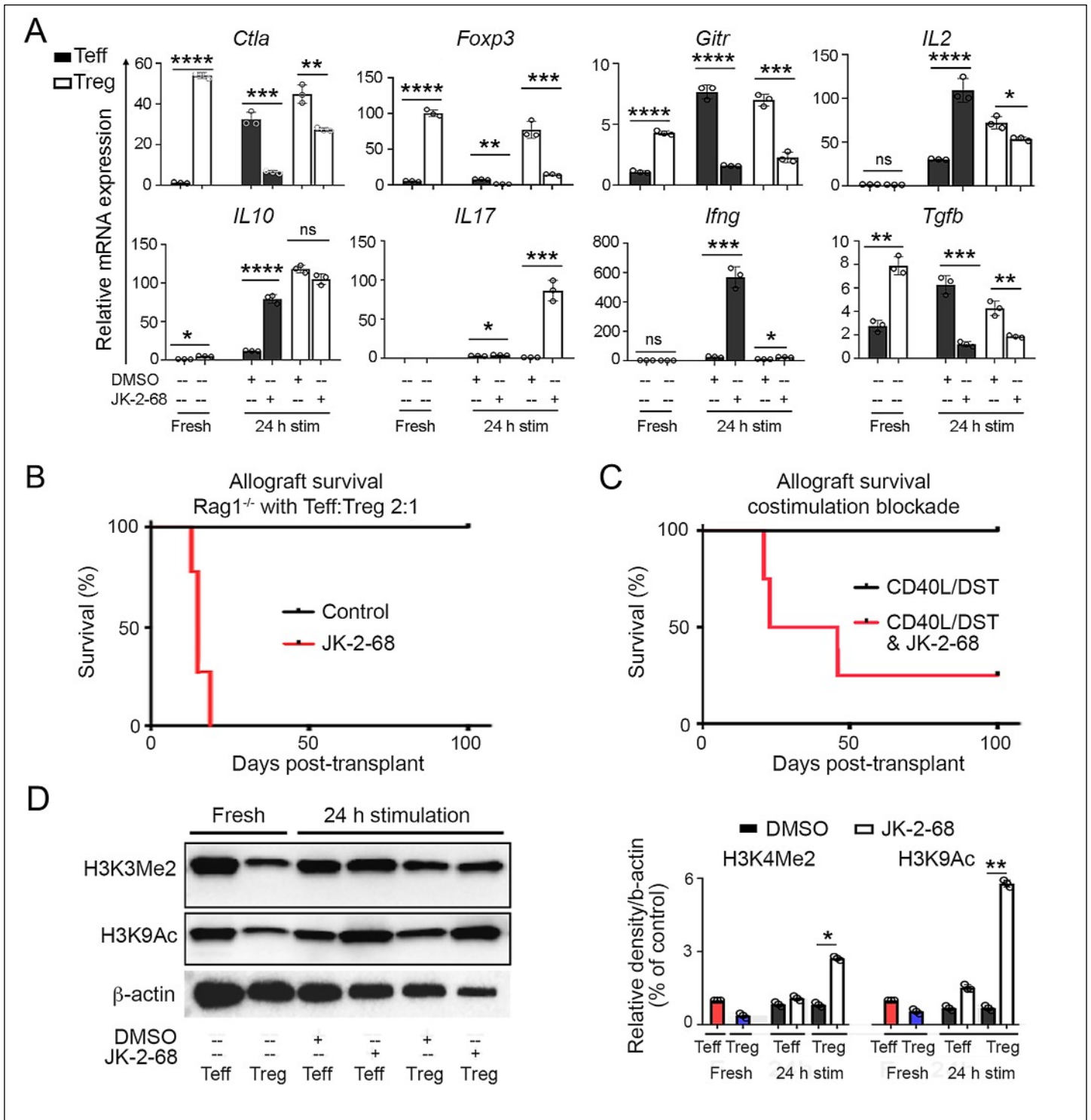


Figure 7. CoREST complex inhibitor affects Treg gene expression and function in vitro and in vivo. (A) qPCR analyses of indicated gene expression in T effector and Treg cells. qPCR data were normalized to 18S (* $p < 0.05$, ** $p < 0.01$, *** $p < 0.001$, **** $p < 0.0001$ vs. WT control), and data (mean \pm SD) are representative of 2 independent experiments involving 5 mice/group. (B) Immediately after cardiac allografting from BALB/c donors, recipient C57BL/6 Rag1^{-/-} mice (5 mice/group) were adoptively transferred with 1 million B6 Teffs and 0.5 million B6 Tregs, and treated with or without JK-2-68 (10 mg/kg/d, 14 d); $p < 0.01$ for 2 groups. (C) B6 recipients were transplanted with BALB/c cardiac allografts (5 mice/group) and treated with CD40L mAb (200 μ g)/DST and JK-2-68 (10 mg/kg/d, 14 d); $p < 0.01$ for 2 groups. (D) Representative bands (left) and statistical analysis (Right) of Western blotting for H3K4Me2 and HK9Ac expression in fresh Tregs or Treg stimulated for 24 hours by CD3/CD28 mAb-coated beads with or without JK-2-68 (10 μ M).

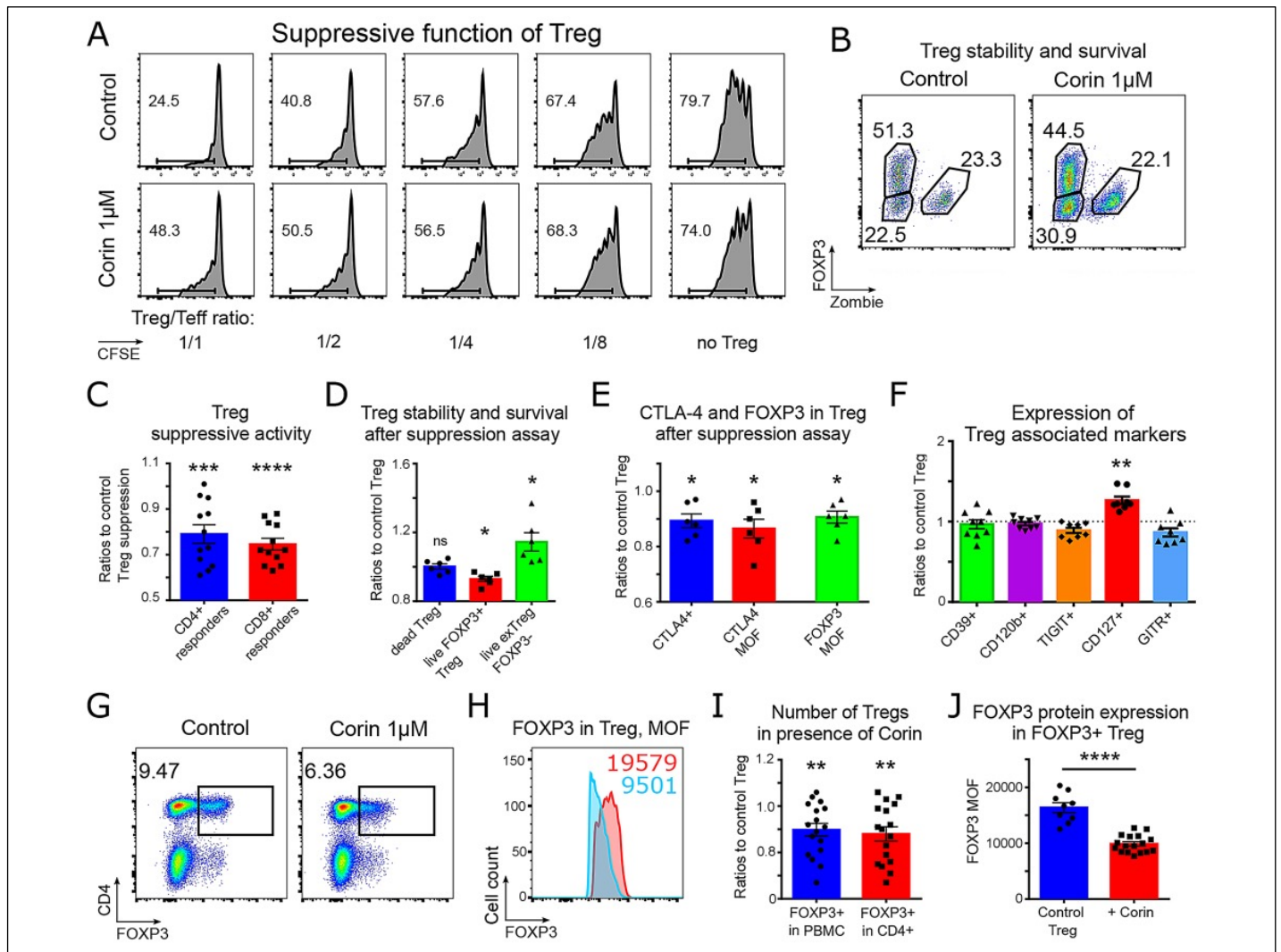


Figure 8. Effects of CoREST complex inhibitor on human Treg cells. (A) Human healthy donor Tregs were incubated with Corin (1 μ M) for 2.5 h, washed twice and incubated with CFSE-labeled, anti-CD3 ϵ microbead-stimulated healthy donor PBMC cells for 5-6 d. Representative data shows impaired Treg suppressive function for CD4⁺ responder cells (CD8⁺ responder cells in Suppl. Figure 8). (B) After suppression assays, cells were stained with fixable live/dead marker Zombie Yellow and FOXP3, cells were gated into CD4⁺CFSE⁻Zombie⁺ (=dead Treg), CD4⁺CFSE⁻Zombie⁻Foxp3⁻ (=live exTreg), and CD4⁺CFSE⁻Zombie⁻Foxp3⁺ (=live Treg), to evaluate Treg stability (loss of FOXP3) and survival (% of Zombie⁻ cells). (C) Statistical analysis of data shown in panel A; Tregs from 5 healthy donors Treg and responder PBMC from 3 healthy donors were tested in 5 independent experiments (total of 12 suppression assays). Treg ability to suppress divisions of CD4⁺ and CD8⁺ responders were analyzed separately, one sample T-test with theoretical mean = 1. (D) Statistical analysis of data from panel B; data from 6 assays are pooled, Wilcoxon signed ranked test. (E) Cells were stained for Zombie Yellow, FOXP3 and CTLA-4. Viable CD4⁺CFSE⁻Zombie⁻FOXP3⁺ Tregs were gated and evaluated for CTLA-4 expression (MOF, % of positive cells) and FOXP3 MOF. Data were pooled from 6 assays, Wilcoxon signed ranked test. (F-J) Healthy donors PBMC (from 5 different donors in 3 experiments) were incubated with Corin (1 μ M) and stimulated overnight with CD3 ϵ /CD28 mAb-coated beads (1.3 beads/cell). (F) TIGIT and GITR expression tended to be decreased in viable CD4⁺FOXP3⁺ Treg, but without significance, whereas CD127 expression significantly increased in presence of Corin. (G) Representative example of FOXP3 expression in PBMC and (H) FOXP3 MOF in viable CD4⁺FOXP3⁺ Treg. (I, J) statistics showing (I) decreased Treg numbers and (J) decreased MOF of FOXP3 in human Treg treated with Corin. All tests in (F) to (I) are one sample t-tests with Bonferoni correction for multiple comparisons, whereas (J) was evaluated by unpaired t-test. P-values, * p <0.05, ** p <0.01, *** p <0.001, **** p <0.0001. Data shown as mean \pm SD.

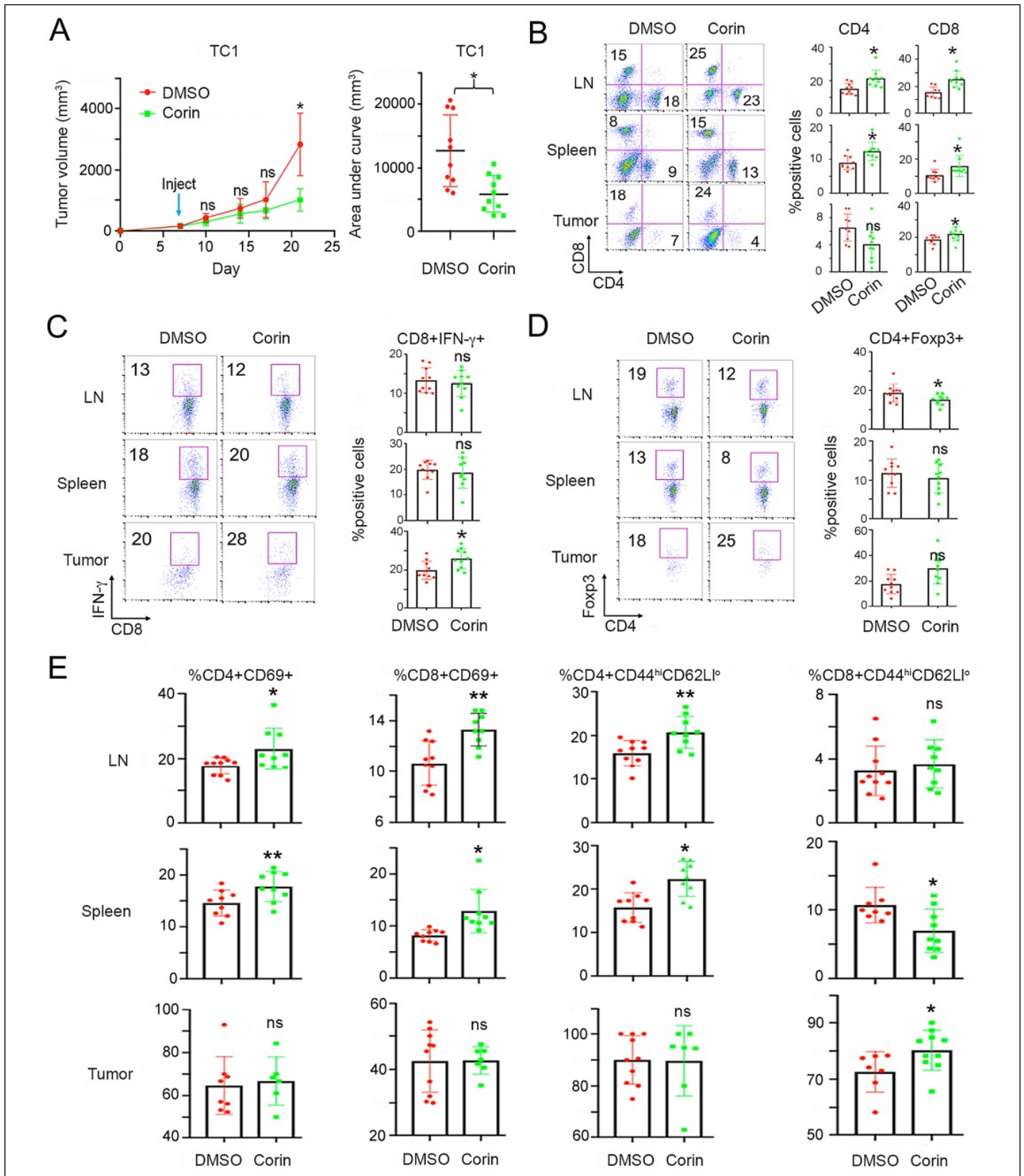


Figure 9. CoREST complex inhibitor enhances anti-tumor immunity. (A) TC1 tumor volumes and area-under-curve data were smaller in C57BL/6 mice treated with corin (10 mg/kg/day) vs. DMSO (n=8-10/group). Analysis of the percentages of (B) CD4⁺ and CD8⁺ cells, (C) CD8⁺IFN- γ ⁺ cells, (D) CD4⁺Foxp3⁺ cells, and (E) T cell activation markers (CD8⁺CD69⁺, CD4⁺CD69⁺, CD4⁺CD44^{hi}CD62L^{lo}, CD8⁺CD44^{hi}CD62L^{lo}) in lymph nodes, spleens and tumors from corin and DMSO-treated groups. Data are shown as mean \pm SD, 8-10 samples/group. Student's t-test for unpaired data; *p<0.05, **p<0.01 or ns (not significant) vs. control.

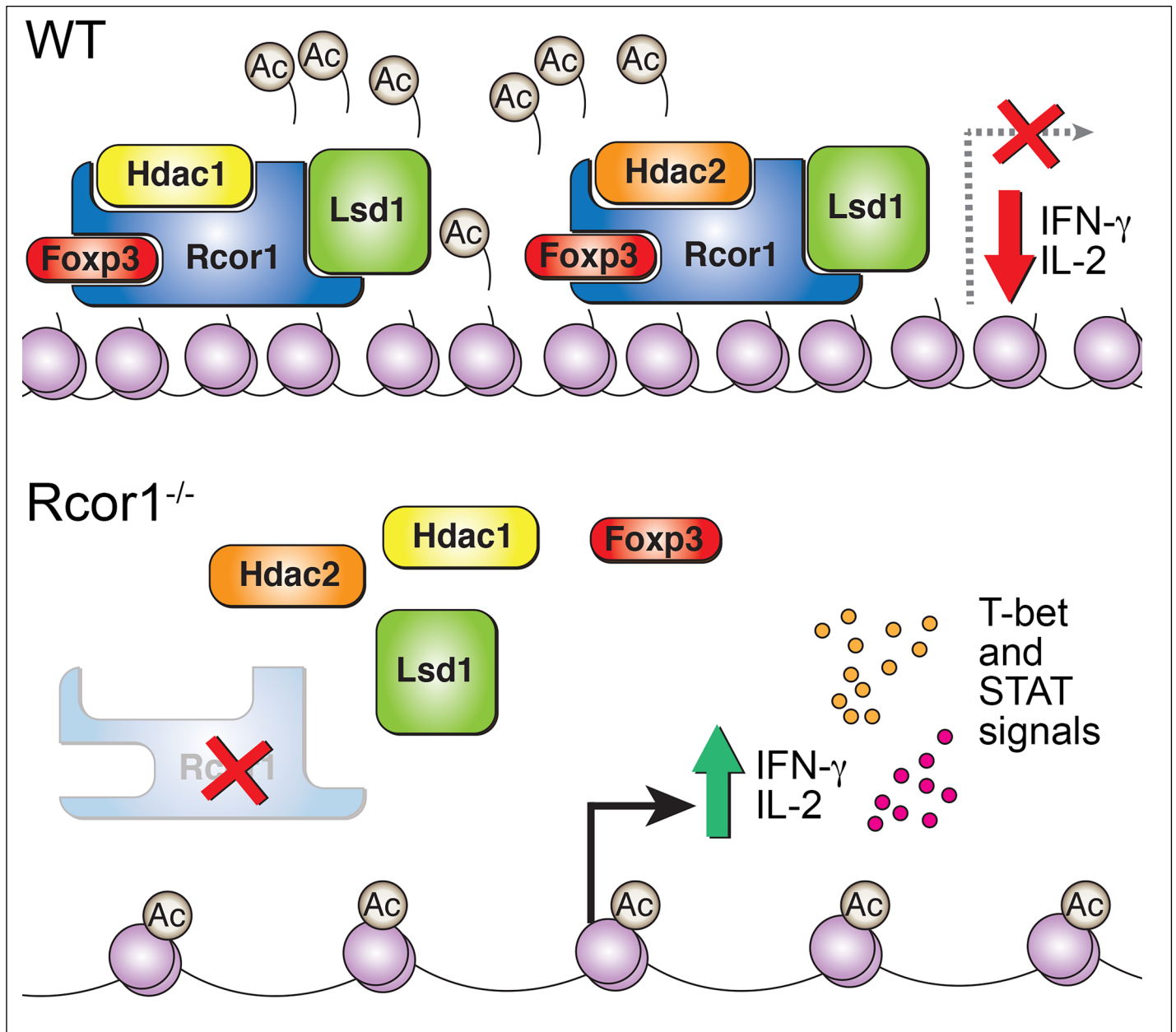


Figure 10. Schematic of the actions of the CoREST complex in Foxp3⁺ Treg cells. In WT cells, Foxp3 recruits the CoREST complex, consisting of Rcor1, Hdac1 or Hdac2, and Lsd1, to repress expression of multiple genes, including IL-2 and IFN- γ . In the absence of Rcor1, recruitment of the CoREST complex by Foxp3 is markedly impaired, leading to derepression of multiple genes, including those encoding IL-2 and IFN- γ , and downstream signaling molecules, such as T-bet and STAT1.